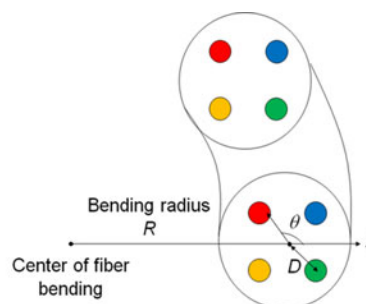# Crosstalk Analysis of Heterogeneous Multicore Fibers Using Coupled-Mode Theory

**Takeshi Fujisawa,** *Member, IEEE*
**Yoshimichi Amma**
**Yusuke Sasaki**
**Shoichiro Matsuo,** *Member, IEEE*
**Kazuhiko Aikawa**
**Kunimasa Saitoh,** *Member, IEEE*
**Masanori Koshiba,** *Fellow, IEEE*
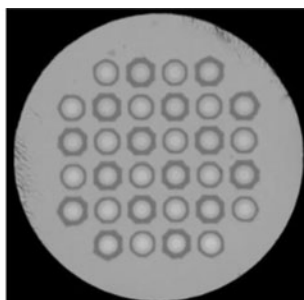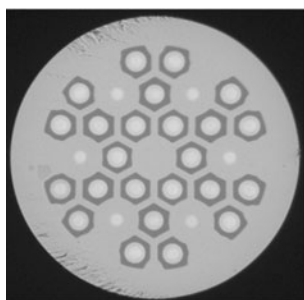
# Crosstalk Analysis of Heterogeneous Multicore Fibers Using Coupled-Mode Theory

**Takeshi Fujisawa,[1]** *Member, IEEE*, **Yoshimichi Amma,[2]**
**Yusuke Sasaki,[2] Shoichiro Matsuo,[2]** *Member, IEEE*,
**Kazuhiko Aikawa,[2] Kunimasa Saitoh,[1]** *Member, IEEE*,
**and Masanori Koshiba,[1]** *Fellow, IEEE*

[1]Graduate School of Information Science and Technology, Hokkaido University, Sapporo
060-0814, Japan
[2]Fujikura Ltd., Chiba 285-8550, Japan

**Abstract:** Intercore crosstalk of heterogeneous multicore fiber is investigated based on coupled-mode theory. Random twisting model is used for estimating the crosstalk. The crosstalk of two kinds of fibers: triangular lattice 30-core fiber with four kinds of cores and square lattice 32-core fiber with two kinds of cores is investigated both theoretically and experimentally. Unlike previous study, measured crosstalk for all the combinations of cores for both fibers is in good agreement with calculated values with single correlation length, showing the validity of the theoretical model used here.

**Index Terms:** Heterogeneous multicore fiber, coupled-mode theory, intercore crosstalk.

## 1. Introduction

Space-division-multiplexing (SDM) is an attractive technology for increasing the network capacity. Multicore fibres (MCFs) are one of the transmission media for SDM and various designs of MCFs have been intensively studied [1]. When the cores in MCF are all the same, it is called homogeneous MCF and When they are different, it is called heterogeneous MCF (HMCF). One of the major design objectives for MCFs is intercore crosstalk. The crosstalk has to be suppressed below the certain value required by the modulation format of the signal [2]. An HMCF is a promising candidate for SDM transmission because the intercore crosstalk can be suppressed due to the phase mismatch between adjacent cores.

To quantify the crosstalk in MCFs, theoretical methods based on a coupled-mode theory (CMT) [3]–[5], and coupled-power theory (CPT) [5], [6] were proposed. In refs [4]–[6], the fibers are assumed to be uniformly bent with the constant bending radius ($R$) and uniformly twisted with the constant twisting rate. It was shown in ref [5] that both CMT and CPT give almost the same results for the same fiber model. In addition, giving random phase offset at each correlation length, the crosstalk of quasi-homogeneous MCF [4], [7] was successfully explained with a single fitting
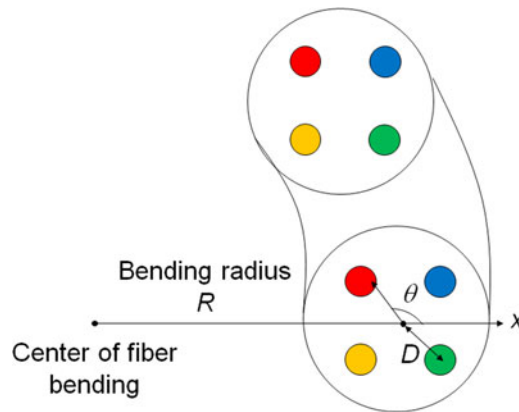
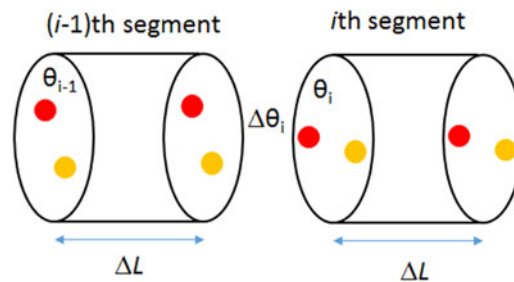Fig. 1. A schematic of bent fiber and parameters used for modeling.



Fig. 2. A schematic of twisting model.

parameter (correlation length). Here, the correlation length in [4], [7] was defined as the length in which the phase of the light is preserved. These models have been widely used for the analysis of various MCF crosstalk.

Recently, we fabricated 30-core HMCF [8]. The fiber has four kinds of cores and they are heterogeneously arranged in triangular lattice layout. The crosstalk was analysed by CPT and the correlation lengths for each core combinations, which explain measured results well, range from 1 to 1000 m. Although the correlation length for different core combinations do not have to be the same, three order difference is not likely to occur. Therefore, more general theoretical model for the analysis of crosstalk in HMCFs is strongly desired.

In this paper, the intercore crosstalk of HMCF is investigated based on coupled-mode theory. Random twisting model is used for estimating the crosstalk. The crosstalk of two kinds of fibers: triangular lattice 30-core fiber with 4 kinds of cores and square lattice 32-core fiber with two kinds of cores is investigated both theoretically and experimentally. Unlike previous study [8], measured crosstalk for all the combinations of cores for both fibers is in good agreement with calculated values with single correlation length. These results indicate that incorporating longitudinal random twisting state is crucial for the analysis of the crosstalk of HMCF.

## 2. Coupled-Mode Theory

Figs. 1 and 2 show the schematic of random twisting models. In this paper, $z$ is the propagation direction and $xy$-plane is the transverse plane. We consider the fiber is uniformly bent to x direction with the constant bending radius of $R$. The fiber with the length of $L$ is divided into $M$ segments with the length of $\triangle L$. In [4]–[6], it was assumed that the fiber is uniformly twisted with constant twisting rate and random phase offset is manually inserted at every correlation length. The phase offset is between 0 and $2\pi$ and given with equal probability for all values (completely random). Here, we assume that the fiber has longitudinally random twisting. Each segment has randomly generated
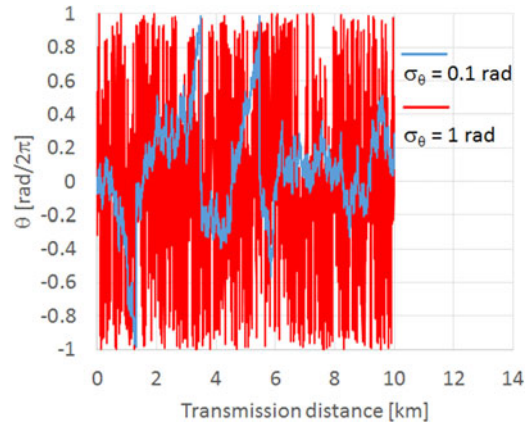
Fig. 3. Longitudinal twisting angle distributions.

twisting angle $\Delta\theta_i$ relative to the previous segment as shown in Fig. 2. $\Delta\theta_i$ has Gaussian distribution with the mean value of 0 rad and the standard deviation of $\sigma_\theta$ rad. Therefore, twisting angle of $i$th segment is $\theta_{i-1} + \Delta\theta_i$. We assume the fiber structure is uniform within one segment. The twisting angle difference between each segment corresponds to the random phase offset in the previous work. However, since $\Delta\theta_i$ has Gaussian distribution, the randomness (phase offset) is not given with equal probability as in the previous studies [4]–[6]. This point is the main difference in the fiber model compared with the previous studies. Fig. 3 shows one example of twisting angle $\theta(/2\pi)$ as a function of $L$ for the fiber with $\Delta L = 1$ m. Twisting angle is randomly distributed over $-2\pi$ to $2\pi$. For large $\sigma_\theta$, the number of twisting is very large. Assuming random twisting is more realistic for the fiber with no special treatment for coiling.

The $N$-mode coupled-mode equation is given by

$$\frac{d\boldsymbol{a}}{dz} = -j\boldsymbol{A}\boldsymbol{a} \tag{1}$$

where $\boldsymbol{a} = [a_1, a_2, \cdots a_N]^T$ is a column vector of the field amplitude of each mode. $\boldsymbol{A}$ is a matrix given by

$$\boldsymbol{A} = \begin{bmatrix} \beta_1 & \kappa_{12} & \cdots & \kappa_{1N} \\ \kappa_{21} & \beta_2 & & \vdots \\ \vdots & & \ddots & \vdots \\ \kappa_{N1} & \cdots & \cdots & \beta_N \end{bmatrix} \tag{2}$$

where $\beta_m$ is the propagation constant of $m$th core, and $\kappa_{mn}$ is symmetrized coupling coefficient [5] between $m$th and $n$th cores and $\kappa_{mn} = \kappa_{nm}$. The equation of the coupling coefficient can be found in, for example, [9]. Effective index of $m$th core at $i$th step is given by [4], [5], [10]

$$n_{eff,m,i} = n_{eff,m}\left(1 + \frac{D_m \cos\theta_{m,i}}{R}\right) \tag{3}$$

where $D_m$ is the distance between the center of the fiber and the center of $m$th core, $n_{eff,m}$ is the effective index of $m$th core without bending and twisting. The definitions of the parameters are shown in Fig. 1.
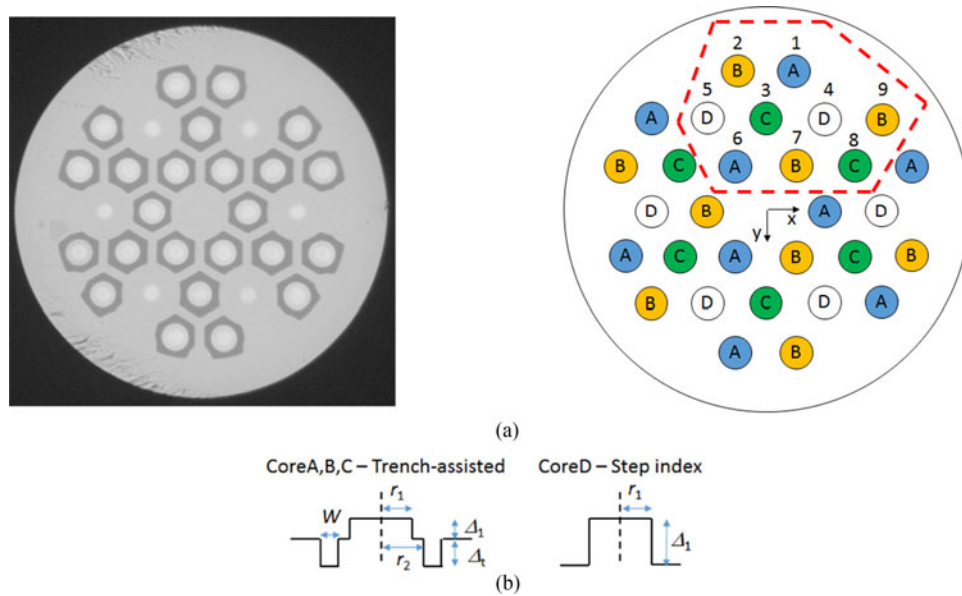
Fig. 4. (a) A microscope picture and cross-sectional structure of 30-core HMCF and (b) core index profile.

Since the matrix $A$ is symmetric, we can diagonalize it with the matrix $P$ as

$$D = P^{-1}AP = \begin{bmatrix} \lambda_1 & 0 & \cdots & 0 \\ 0 & \lambda_2 & & \vdots \\ \vdots & & \ddots & \vdots \\ 0 & \cdots & \cdots & \lambda_N \end{bmatrix} \tag{4}$$

where $\lambda_i$ is the eigenvalue of the matrix $A$ and $P$ contains eigenvectors of $A$. Substituting (4) into (1) yields

$$\frac{da}{dz} = -jPDP^{-1}a \tag{5}$$

Multiplying $P^{-1}$ from the left side and recall the structure is assumed to be uniform within one segment, one obtains

$$\frac{dy}{dz} = -jDy \tag{6}$$

where $y = P^{-1}a$. Equation (5) can be solved analytically because $D$ is diagonal and $a$ is obtained from $y$.

## 3. Results

### 3.1 Triangular Lattice 30-Core HMCF With Four Kinds of Cores

Fig. 4(a) shows a microscope picture and cross-sectional structure of 30-core HMCF [8]. It consists of four kinds of cores. Cores A, B, and C have trench-assisted (TA) index profile and core D has step index profile as shown in Fig. 4(b). The step index core is used to obtain large effective index difference compared with TA index core. Core parameters are summarized in Table 1. All the measurements and calculations are done for the wavelength of 1.55 $\mu$m. The crosstalk was measured by wavelength sweeping method [11] and a TA-SMF was used for the input and output

Table 1

Core Parameters of 30-Core HMCF

| | $r_1$ [$\mu$m] | $\triangle_1$ [%] | $r_2/r_1$ | $W/r_1$ |
|---|---|---|---|---|
| Core A | 4.76 | 0.338 | 1.7 | 1.0 |
| Core B | 4.62 | 0.305 | 1.7 | 1.0 |
| Core C | 4.47 | 0.273 | 1.7 | 1.2 |
| Core D | 4.68 | 0.388 | – | – |

Table 2

Correlation Lengths for All Core Combinations Estimated by CPT [8]

| Combination | $\triangle n_{\text{eff}}$ | $\triangle L$ [m] |
|---|---|---|
| Core A-B | 0.00051 | 1 |
| Core A-C | 0.001 | 10 |
| Core A-D | 0.00063 | 100 |
| Core B-C | 0.0005 | 10 |
| Core B-D | 0.00113 | >600 |
| Core C-D | 0.00163 | >1000 |

fibres. By using the method, we can improve the dynamic range of crosstalk to about 70 dB. The fiber length is 9.6 km and long length fiber is preferable for the crosstalk measurement of HMCFs since the crosstalk is too small for short length fiber.

Table 2 shows $\triangle n_{eff}$ and the correlation length for all the combinations of cores estimated by CPT (see [8] for detail). The estimated length ranges from 1 to 1000 m. Although the correlation length does not have to be the same for different core combinations, three order difference in the length is not likely to occur. We calculated the crosstalk of this fiber using CMT with random twisting model described in the previous section. To reduce the computational cost, 9 cores shown in Fig. 4(a) are considered and the light is launched to one of the cores. We numerically confirmed that the crosstalk to the cores in the second ring is negligible (for example, when the light is launched to core1, the second ring cores are 5 to 9), and therefore, the 9-core model is valid for the crosstalk analysis of 30-core fiber if the light is launched to core 1 to 4. The numerical crosstalk is averaged over 100 fiber realizations. Fig. 5 shows optical powers in core 1 to 9 as a function of $L$ for $R = 155$ mm. The light is launched to core 1 and $\sigma_\theta = 1$ rad and $\triangle L = 1$ m. The crosstalk is accumulated with the distance and the values for "second ring" core (in this case, cores 5 to 9) are below $-100$ dB and negligible, showing the validity of using 9-core model.

Hereafter, we denote the crosstalk between core $m$ and $n$ when light is launched to core $m$ as "$XT_{m,n}$". Fig. 6(a), (b), and (c) show $XT_{1,3}$ (Core A-C), $XT_{2,3}$ (Core B-C), and $XT_{3,4}$ (Core C-D) as a function of $\triangle L$ for $R = 155$ mm and different values of $\sigma_\theta$. The crosstalk is increased for large $\sigma_\theta$ and short $\triangle L$ due to the increased randomness. Two horizontal dashed lines in each Figure show maximum and minimum measured crosstalk. For $\sigma_\theta = 1$ rad and $\triangle L = 1$ m, measured crosstalk for all the combinations are well explained. Fig. 7(a), (b), and (c) show crosstalk as a function
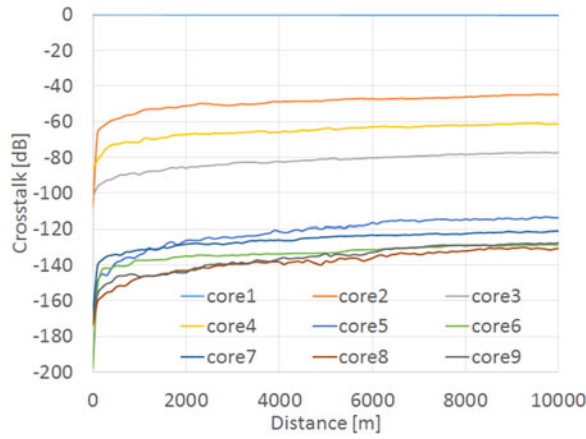
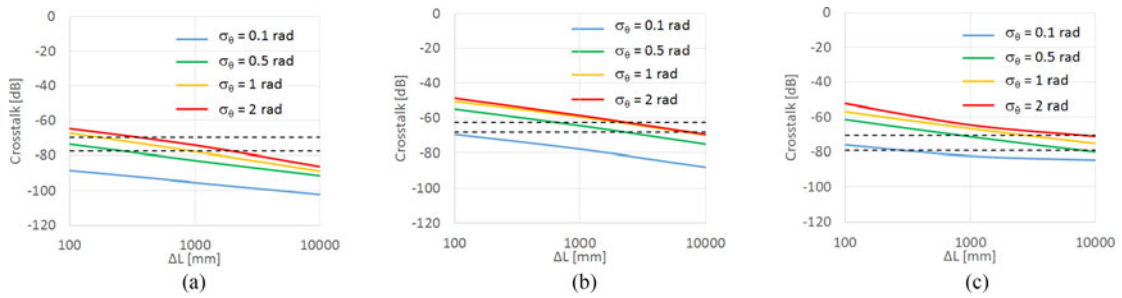Fig. 5. Optical powers at each core as a function of transmission distance for $R = 155$ mm.



Fig. 6. (a) XT1, 3 (Core A-C), (b) XT2, 3 (Core B-C), and (c) XT3, 4 (Core C-D) as a function of _L for $R = 155$ mm and different values of $\sigma\sigma_\theta$.
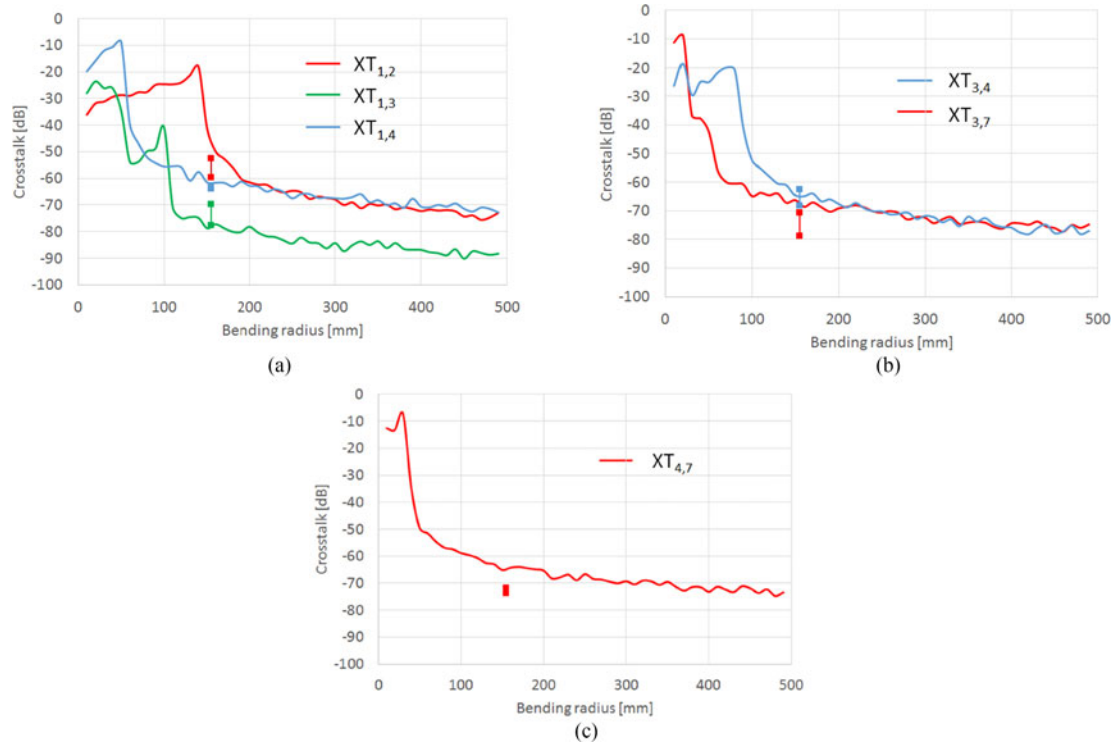


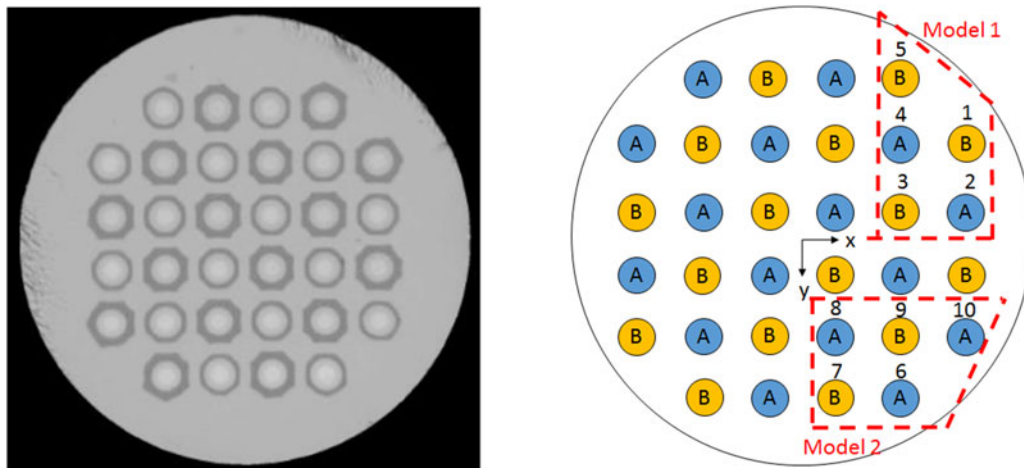Fig. 7. (a) $XT_{1,2}$, $XT_{1,3}$, $XT_{1,4}$, (b) $XT_{3,4}$, $XT_{3,7}$, and (c) $XT_{4,7}$ as a function of $R$.

Fig. 8. A microscope picture and cross-sectional structure of 32-core HMCF.

Table 3

Core Parameters of 32-Core HMCF

|         | $r_1$ [$\mu$m] | $\Delta_1$ [%] | $r_2/r_1$ | $W/r_1$ |
|---------|------|------|-----|------|
| Core A  | 4.80 | 0.35 | 1.7 | 0.58 |
| Core B  | 4.65 | 0.31 | 1.7 | 1.0  |

of bending radius when the light is launched to core 1, 3, and 4, respectively, for $\sigma_\theta = 1$ rad and $\Delta L = 1$ m. In Fig. 7(a), $XT_{1,2}$, $XT_{1,3}$, $XT_{1,4}$, in Fig. 7(b), $XT_{3,4}$, $XT_{3,7}$, and in Fig. 7(c), $XT_{4,7}$ are shown (all six combinations) together with measured results at $R = 155$ mm. Calculated results for all the combinations are in good agreement with measured results with single correlation length and without manually inserted random phase offset, showing the validity of the model.

### 3.2 Square Lattice 32-Core HMCF With Two Kinds of Cores

Fig. 8 shows a microscope picture and cross-sectional structure of 32-core HMCF [12]. It consists of two kinds of cores and they are placed in square lattice. Both cores A and B have TA index profile as shown in Fig. 4(b) and core parameters are summarized in Table 3. The fiber length is 51.4 km and the wavelength is 1.55 $\mu$m. We consider 5-core model shown in Fig. 8 to reduce the computational cost. When light is launched from core A (B), 5-core model 2 (1) is used. Fig. 9(a), (b), and (c) show $XT_{6,8}$ (Core A-A), $XT_{6,7}$ (Core A-B), and $XT_{1,3}$ (Core B-B) as a function of $\Delta L$ for $R = 155$ mm and different values of $\sigma_\theta$. Two horizontal dashed lines in each Figure show maximum and minimum measured crosstalk. For the same core combinations (Core A-A or Core B-B), the crosstalk values are almost independent on $\sigma_\theta$ and $\Delta L$. This is because that there are phase matching points in the fiber, at which the effective indexes of both cores are equal, and these points dominate the crosstalk. The calculated values are in good agreement with the measured values for both combinations. For different core combination (Core A-B), the crosstalk is increased for large $\sigma_\theta$ and short $\Delta L$ due to the increased randomness as in the case of 30-core fiber. For $\sigma_\theta = 1$ rad and $\Delta L = 1$ m, calculated and measured crosstalk are well matched. This fitting parameter combination ($\sigma_\theta$, $\Delta L$) = (1 rad, 1 m) is the same as in the case of 30-core fiber.
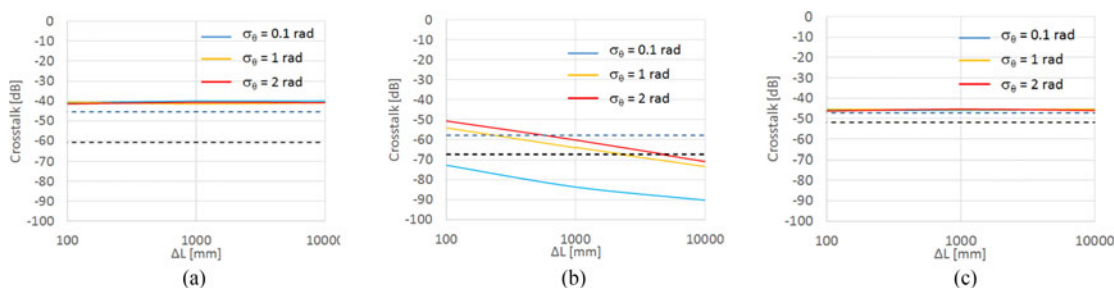
Fig. 9. (a) $XT_{6,8}$ (Core A-A), (b) $XT_{6,7}$ (Core A-B), and (c) $XT_{1,3}$ (Core B-B) as a function of $\Delta L$ for $R = 155$ mm and different values of $\sigma_\theta$.

Since two different fibers fabricated by the same manufacturer have the same fitting parameters, the calculated results seem to be very reasonable.

Finally, we consider the number of rotation of the fiber for above fitting parameter. Since in the random twisting model, the direction of twisting is also random, we cannot define uniform twisting rate. Here, instead, we count the point where the rotation angle $\theta$ exceeds $|2\pi|$ in the fiber. For example, in Fig. 3, the number of rotation is 3 for the fiber with $\sigma_\theta = 0.1$ rad and $\Delta L = 1$ m. Therefore, effective rotation rate is about $3/1000 \simeq 0.003$ rotation per m. We count this effective rotation rate for the fiber with specific $\sigma_\theta$ and $\Delta L$ for 100 realizations and take the average. For $(\sigma_\theta, \Delta L) = (1$ rad, $1$ m$)$, the effective rotation rate is 0.13 rad/m, or, 1 rotation per 50 m. The value is reasonable for the naturally coiled fiber.

## 4. Conclusion

We investigated the intercore crosstalk of HMCF using CMT. Two kinds of HMCF fabricated by the same manufacturer were used and investigated in detail both theoretically and experimentally. By assuming longitudinal random twisting, measured crosstalk values are in good agreement with calculated results with single correlation length and without manually inserted random phase offset. The combinations of fitting parameters for explaining the measured results are the same for different fibers. Therefore, the presented model is very useful for estimating the crosstalk of HMCF.

## References

[1] K. Saitoh and S. Matsuo, "Multicore fiber technology," *J. Lightw. Technol.*, vol. 34, no. 1, pp. 55–66, Jan. 2016.
[2] P. J. Winzer, "High-spectral-efficiency optical modulation formats," *J. Lightw. Technol.*, vol. 30, no. 24, pp. 3824–3835, Dec. 2012.
[3] J. M. Fini, B. Zhu, T. F. Taunay, and M. F. Yan, "Statistics of crosstalk in bent muticore fibers," *Opt. Exp.*, vol. 18, no. 14, pp. 15122–15129, Jun. 2010.
[4] T. Hayashi, T. Nagashima, O. Shimakawa, T. Sasaki, and E. Sasaoka, "Crosstalk variation of multi-core fibre due to fibre bend," *Proc. 36th Eur. Conf. Exhib. Opt. Commun.*, Torino, 2010, Paper We.8.F.6.
[5] M. Koshiba, K. Saitoh, K. Takenaga, and S. Matsuo, "Multi-core fiber design and analysis: Coupled-mode theory and coupled-power theory," *Opt. Exp.*, vol. 19, no. 26, pp. B102–B111, Dec. 2011.
[6] M. Koshiba, K. Saitoh, K. Takenaga, and S. Matsuo, "Analytical expression of average power-coupling coefficients for estimating intercore crosstalk in multicore fibers," *IEEE Photon. J.*, vol. 4, no. 5, pp. 1987–1995, Oct. 2012.
[7] S. Matsuo *et al.*, "Crosstalk behaviour of cores in multi-core fiber under bent condition," *IEICE Electron. Exp.*, vol. 8, no. 6, pp. 385–390, Mar. 2011.
[8] Y. Amma *et al.*, "High-density multicore fiber with heterogeneous core arrangement," *Proc. Opt. Fiber Commun. Conf. Exhib.*, Los Angeles, CA, USA, 2015, Paper Th4C.4.
[9] K. Okamoto, *Fundamentals of Optical Waveguides*. New York, NY, USA: Academic Press, 2006.
[10] D. Marcuse, "Influence of curvature on the losses of doubly clad fibers," *Appl. Opt.*, vol. 21, no. 23, pp. 4208–4213, Dec. 1982.
[11] T. Hayashi, T. Taru, O. Shimakawa, T. Sasaki, and E. Sasaoka, "Characterization of crosstalk in ultra-low-crosstalk multi-core fiber," *J. Lightw. Technol.*, vol. 30, no. 4, pp. 583–589, Feb. 2012.
[12] Y. Sasaki *et al.*, "Crosstalk-managed heterogeneous single-mode 32-core fibre," in *Proc. 42nd Eur. Conf. Opt. Commun.*, Dusseldorf, Germany, 2016, pp. 550–552.